ACS APPLIED MATERIALS & INTERFACES

Research Article

www.acsami.org

Gamma-Irradiated Carbon Nanotube Yarn As Substrate for High-Performance Fiber Supercapacitors

Fenghua Su,[†,‡] Menghe Miao,*[,‡] Haitao Niu,[§] and Zhixiang Wei[⊥]

[†]School of Mechanical and Automotive Engineering, South China University of Technology, Guangzhou 510641, P. R. China

[‡]CSIRO Materials Science and Engineering, Belmont, Victoria 3216, Australia

[§]Institute for Frontier Materials, Deakin University, Waurn Ponds, Victoria 3216, Australia

[⊥]National Center for Nanoscience and Technology, Beijing 100190, P. R. China

Supporting Information

ABSTRACT: As an electrical double layer capacitor, dry-spun carbon nanotube yarn possesses relatively low specific capacitance. This can be significantly increased as a result of the pseudocapacitance of functional groups on the carbon nanotubes developed by oxidation using a gamma irradiation treatment in the presence of air. When coated with high-performance polyaniline nanowires, the gamma-irradiated carbon nanotube yarn acts as a high-strength reinforcement and a high-efficiency current collector in two-ply yarn supercapacitors for transporting charges generated along the long electrodes. The resulting supercapacitors demonstrate excellent electrochemical performance, cycle stability, and resistance to folding−unfolding that are required in wearable electronic textiles.

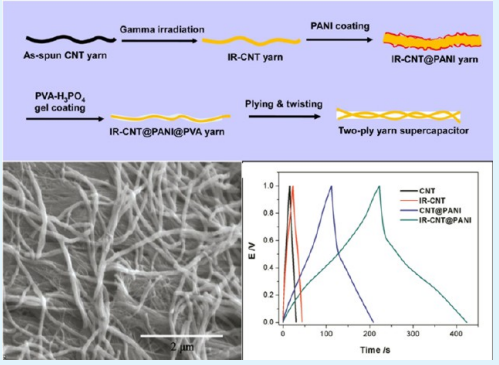

KEYWORDS: *gamma irradiation, carbon nanotubes, polyaniline nanowires, fiber supercapacitors*

1. INTRODUCTION

Consumer electronic devices are becoming smaller and more portable and are increasingly being combined with the cloth system. Wearable electronic textiles demand for the development of flexible, lightweight, and safe energy storage devices. The flexible energy storage devices currently under development may be planar (film or thin block) or linear (fiber or yarn).[1−4] Although many of these devices have achieved high electrochemical performances, they are generally based on materials that are not strong or flexible enough to sustain the stresses experienced in textile manufacture and daily use.[3,5] Planar flexible energy storage devices do not allow sweat and air to pass through freely and therefore do not meet the wearer comfort requirements for wearable electronic textiles. Linear devices (fiber and yarn) can be made into woven and knitted fabrics that contain numerous voids that form passages for air and moisture to pass through. Conventional high strength carbon fibers and high porosity activated carbon fibers have been investigated for use as substrates for fiber supercapacitors.[6−8] However, both carbon fibers and activated carbon fibers cannot serve as normal textile fibers because they are very brittle and will break easily when their resulting fabrics are folded like ordinary textile fabrics.

Carbon nanotubes (CNTs) are attractive electrode materials for developing high-performance supercapacitors due to their high mechanical strength, electrical conductivity, charge transport capability, and electrolyte accessibility.[9−11] The well-defined tube spacing between vertically aligned CNTs in porous arrays (forests) provides high electrolyte accessibility. Vertically aligned multiwalled carbon nanotube (MWCNT) forests can be drawn into continuous webs that may be further converted into yarns by twist insertion, mechanical rubbing and liquid densification.[12,13] The resulting yarns are very strong and flexible for seamlessly weaving and knitting into fabrics. These carbon nanotube yarns have a porous structure and are electrically conductive. In relative terms, as-spun carbon nanotube yarns are three times stronger than conventional cotton yarns[12] and up to 3 orders of magnitude more conductive than conducting polymer films and fibers.[14−17] One approach to further enhancement of the mechanical strength and electrical conductivity of CNT yarns is high degree densification, which nonetheless has an adverse effect on yarn porosity.[12] Another approach for improving the electrical conductivity of CNT yarn proposed recently is plying a thin metal wire (e.g., platinum wire) with the CNT yarn, in which the Pt wire acts as the current collector.[18] The drawbacks of this approach are the heavy weight and high cost of the Pt wire.

Like in conventional carbon materials, the electrical charge storage on carbon nanotubes is primarily capacitive in the electrochemical double layer (ECDL). The capacitance values achieved with pure CNT powders and yarns are much lower than pseudocapacitance materials such as conducting polymers

Received: November 6, 2013
Accepted: January 31, 2014
Published: January 31, 2014

 © 2014 American Chemical Society dx.doi.org/10.1021/am404967x | ACS Appl. Mater. Interfaces 2014, 6, 2553−2560

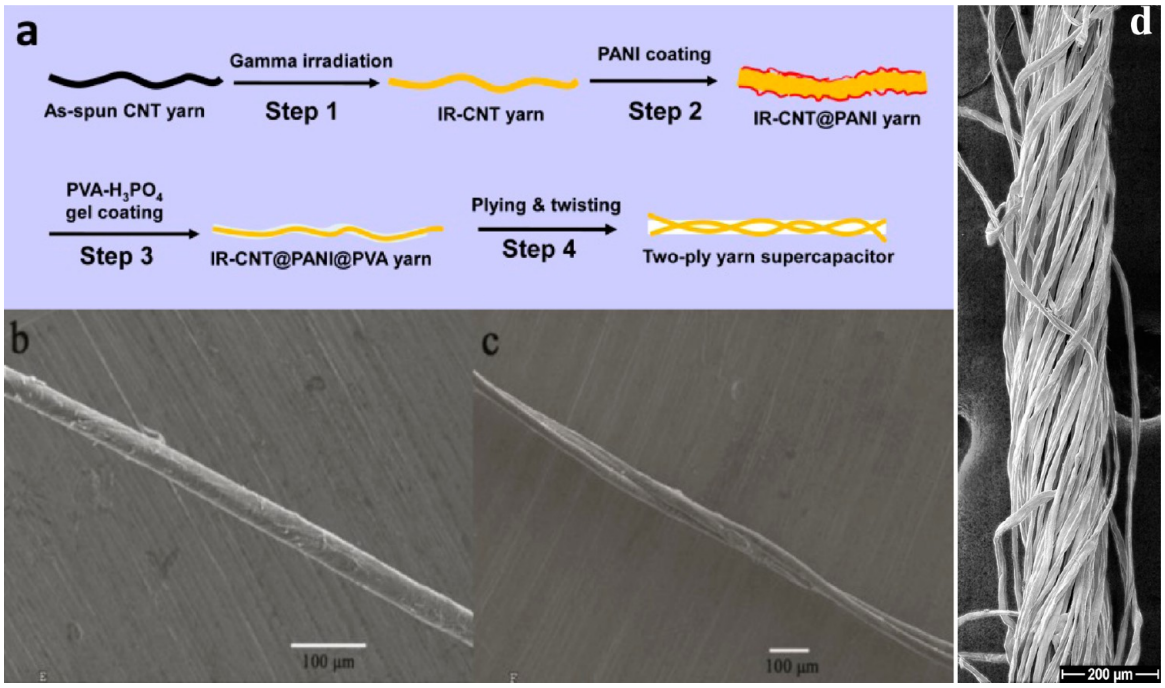

Figure 1. Preparation of IR-CNT@PANI two-ply yarn supercapacitor. (a) Schematic of the preparation procedure. (b) SEM image of IR-CNT@PANI single yarn. (c) SEM image of IR-CNT@PANI two-ply yarn supercapacitor. (d) SEM image of a conventional cotton yarn for comparison.

and metal oxides.[19] In conventional carbon materials, enhancement of capacitance can be reached by utilizing different types of faradaic reactions originating from oxygen and nitrogen heteroatoms in the carbon network.[20] Surface functional groups on activated carbon can be charged and discharged giving rise to pseudocapacitance.[21] Electrochemical, chemical, and cold plasma surface oxidation treatments have been used to treat activated carbon fabrics and demonstrated positive effects on specific capacitance.[22−24] For example, Hsieh and Teng increased the specific capacitance of PAN-based activated carbon fabrics by 25% using a relatively mild oxidative technique.[23] The faradaic current, a direct measure of pseudocapacitance, increased significantly with the extent of oxygen treatment, while the change in double-layer capacitance was only minor.

High energy particle and photon irradiation treatments have been investigated to improve the mechanical and electrical properties of CNT materials, such as buckypapers and yarns, by introducing direct heteroatom or polymer cross-links between CNT shells and between tubes.[25−30] Gamma irradiation of single-walled CNT buckypapers in the presence of air or thionyl chloride resulted in significant increase in mechanical strength and electrical conductivity.[26,28] In a recent study, we demonstrated that the mechanical properties of dry-spun carbon nanotube yarns could be significantly improved by gamma irradiation in the presence of air.[27] X-ray photoelectron spectroscopic analyses revealed that gamma-irradiation significantly increased oxygen concentration and resulted in the emergence of carboxyl groups.

Polyaniline (PANI) nanowires are high pseudocapacitance materials for supercapacitors with large capacitance and capability to charge and discharge at high rates.[31−33] Their main shortcomings are low stability for cyclic charge−discharge, high electrical resistivity for charge transport, and low resistance to repeated mechanical stressing.[34] Carbon nanotube yarns can be used as a strong reinforcement and an effective current collector in fiber supercapacitors based on such high-performance active materials.[34−36]

Here we report a study of the impacts of the gamma irradiation treatment on the electrical conductivity and electrochemical properties of dry-spun carbon nanotube yarns in relation to their application in linear supercapacitors for wearable electronics. The irradiation treatment increased the specific capacitance of the CNT yarns as a result of additional pseudocapacitance attributed to the surface oxygen groups developed in gamma irradiation. The gamma-irradiated CNT yarn significantly improved the electrochemical performance of two-ply yarn supercapacitors on its own and in combination with high-performance polyaniline nanowires.

2. EXPERIMENTAL SECTION

Figure 1a illustrates the fabrication process of the gamma-irradiated CNT yarn/PANI supercapacitor. The as-spun CNT yarn produced from a solid-state multiwalled carbon nanotube forest was treated by gamma irradiation in the presence of air. The gamma-irradiated CNT yarn (IR-CNT) was coated in PANI nanowire suspension (SEM image of IR-CNT@PANI yarn shown in Figure 1b) and subsequently in PVA-H_3PO_4 polymer electrolyte gel. Finally, two ends of the coated yarn were twisted together to form a two-ply yarn supercapacitor. The individual preparation steps are described below. An SEM micrograph of the final IR-CNT@PANI two-ply yarn supercapacitor is shown in Figure 1c.

Some of the preparation steps used to fabricate the IR-CNT@PANI two-ply yarn supercapacitor were omitted to produce simpler types of two-ply yarn supercapacitors for comparison:

- CNT two-ply yarn supercapacitor was produced by coating PVA-H_3PO_4 gel on the as-spun CNT yarn, followed by two-plying the coated yarn.
- IR-CNT two-ply yarn supercapacitor was produced by gamma irradiation of the as-spun CNT yarn, followed by PVA-H_3PO_4 gel coating and two-plying.
- CNT@PANI two-ply yarn supercapacitor was produced by PANI coating and PVA-H_3PO_4 coating of the as-spun CNT yarn, followed by two-plying.

dx.doi.org/10.1021/am404967x | ACS Appl. Mater. Interfaces 2014, 6, 2553−2560

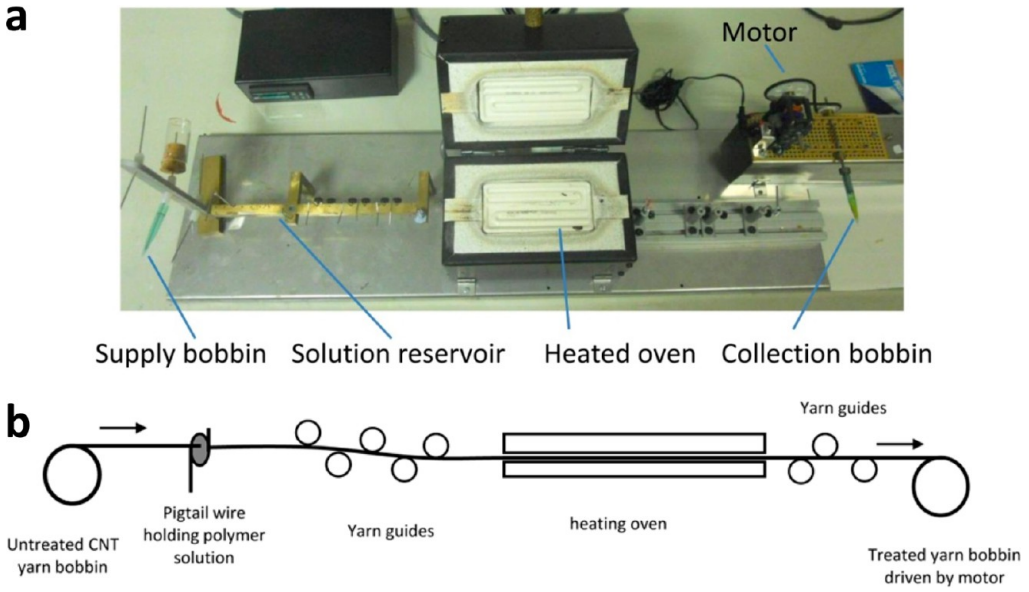

Figure 2. Continuous dip-coating line used for coating polyaniline nanowire solution and PVA-H_3PO_4 gel: (a) photograph, (b) schematic.

2.1. Production of As-Spun Carbon Nanotube Yarn. CNT forests were grown on silicon wafer substrates bearing a thermal oxide layer and iron catalyst coating using chemical vapor deposition (CVD) of acetylene in helium.[37] The resulting CNTs had 7 ± 2 walls with an outer diameter of 10 nm and an inner diameter of 4 nm approximately. The length of the CNTs was found to be approximately 350 μm by measuring the height of the forests. The CNT forests were spun into yarns using an "Up-Spinner" machine reported previously.[38] The CNT yarns were spun to a twist level of 5000 turns per meter using a spindle speed of 5000 rpm.

2.2. Gamma Irradiation Treatment. Gamma irradiation treatment of as-spun CNT yarn in the presence of air was carried out under ambient conditions of approximately 20 °C and 60% RH using a cobalt-60 source which emits 1.17 and 1.33 MeV gamma-rays.[27] The total dose of 600 kGy received by the yarn sample (at a dose rate of 4.2 kGy/h) was recorded by a dose meter placed beside it.

2.3. Preparation of Polyaniline Nanowire Solution. Polyaniline nanowires were synthesized by a reported procedure[31] with some minor modifications. Aniline and potassium biiodate ($KH(IO_3)$) were dissolved at concentrations of 0.1 and 0.0125 M in 1 M HCl, respectively. 36 mL of aniline solution, 40 mL of $KH(IO_3)$ solution and 1 mL of sodium hypochlorite solution (5 wt %, NaClO) were mixed and kept undisturbed at room temperature for 2.5 h. The resulting solution was centrifuged, followed by removing the supernatant. 1 M HCl solutions were added to redissolve the synthesized PANI. After three times of centrifugation, the PANI nanowire solution was obtained.

2.4. Preparation of PVA-H_3PO_4 Gel. 98–99% hydrolyzed polyvinyl alcohol (PVA) with average molecular weight of 57 000–66 000 was supplied by Alfa Aesar. 0.8 g of H_3PO_4 (analytical grade) was added to 10 mL of deionized water with vigorous stirring, and then 1 g of PVA powder was added. The solution was heated up steadily to 90 °C under vigorous stirring until the solution became clear to form the PVA-H_3PO_4 gel.

2.5. Polymer Coating. Coating of PANI and PVA-H_3PO_4 gel was carried out using a home-built continuous coating line shown in Figure 2. The coating line includes a pigtail-shaped reservoir for holding liquid, an electrical heating unit for drying and an electrical motor for controlling yarn throughput speed. The liquid take-up rate and uniformity could be controlled by adjusting the motor speed. Large adjustments of liquid take-up rate can be achieved by varying the viscosity of the polymer solution.

2.6. Characterization. The morphologies of the as-spun CNT yarn and treated yarn samples were characterized by optical microscopy (Olympus) and scanning electron microscopy (SEM, Hitachi S-4800).

Yarn tensile tests were conducted using a Chatillon tensile testing machine equipped with a laser diffraction system for yarn diameter measurement.[38] Electrical conductivity of CNT yarns were measured using a four-probe method.[39] The electrical resistances of CNT yarn specimens were measured at a fixed span length of 50 mm. A constant tension was applied to the yarn specimen during the measurement by hanging a 50 mg mass on each end of the specimen.

Cyclic voltammetry (CV), galvanostatic charge/discharge and electrochemical impedance spectroscopy (EIS) measurements were carried out on a bipotentiostat electrochemical workstation (600D, CH Instruments) using a two-electrode configuration. The specific capacitance of fiber supercapacitor (C_m) was calculated using the formula $C_m = 2I\Delta t/m\Delta V$, where I is discharge current, Δt is discharging time, m is mass of the single yarn (total mass of CNT and PANI if any) in the overlap portion, and ΔV is the voltage drop upon discharging.[40] The EIS used to explore the electrochemical behaviors of the electrode materials was carried out at an amplitude of 5 mV in the frequency range from 500 kHz to 10 mHz.

3. RESULTS AND DISCUSSION

3.1. Effect of Gamma Irradiation on Strength and Conductivity of CNT Yarn. Although the gamma irradiation treatment does not significantly change the CNT packing density in the yarn,[27] it has greatly changed the tensile strength and electrical conductivity of the yarn. The yarn strength increased from 574 to 773 MPa. This translates into a tenacity (specific tensile strength used in the textile industry) of 78.9 cN/tex, or more than three times the tenacity of conventional textile cotton yarns.[41] The high strength IR-CNT yarn and its resulting two-ply yarn supercapacitors would therefore weave and knit well in textile processing. This strength increase is in agreement with our previous findings, which was explained by tube-to-tube cross-linking introduced by gamma irradiation in the presence of oxygen.[27] The CNT structure changes caused by gamma irradiation have been studied.[28,42] With increasing gamma dose, the I_D/I_G ratio of MWCNTs went up sharply first and then went down slowly.[42] Field emission transmission electron microscopy (FE-TEM) showed that gamma irradiation could distort and roughen the walls of MWCNTs.[42]

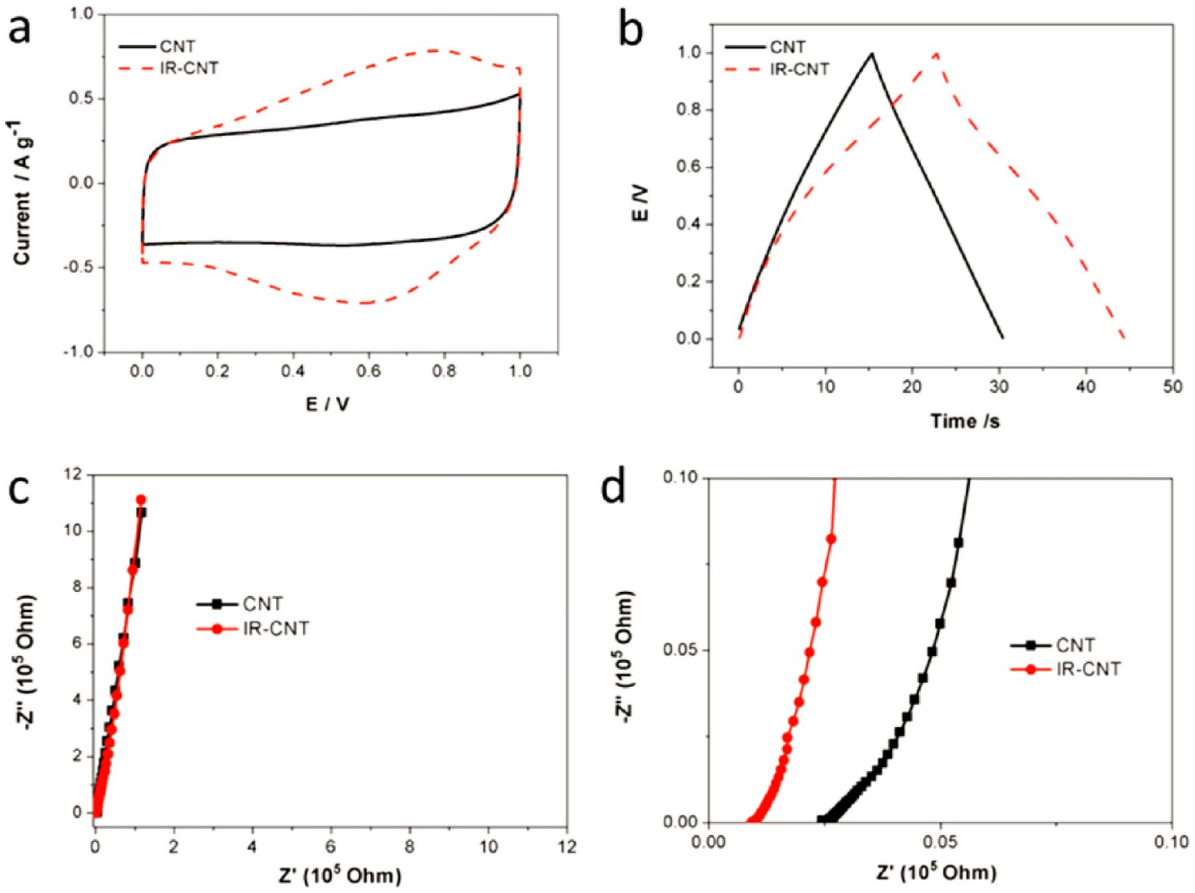

Figure 3. Electrochemical properties of CNT and IR-CNT two-ply yarn supercapacitors. (a) Cyclic voltammographs at 0.1 V s^{-1}. (b) Galvanostatic charge/discharge curves at 0.2 A g^{-1}. (c) Electrochemical impedance spectra. (d) Enlarged electrochemical impedance spectra at high-frequency range.

The IR-CNT yarn also showed a significant increase of electrical conductivity from 35,960 S/m to 54,940 S/m, giving specific conductivities (conductivity divided by yarn bulk density) of 452 and 642 S cm^2 g^{-1}, respectively, representing a 42% increase ascribable to the irradiation treatment.

3.2. Effect of Gamma Irradiation on Electrochemical Performance of CNT Yarn. The electrochemical performances of the two-ply yarn supercapacitors based on CNT and IR-CNT yarns were tested by cyclic voltammetry (CV), galvanostatic charge/discharge and electrochemical impedance spectroscopy (EIS). Figure 3a displays the CV curves of these two supercapacitors measured at the same scan rate 0.1 V· s^{-1} and same potential range from 0 to 1.0 V. The CV curve for the as-spun CNT yarn supercapacitor showed a rounded rectangular shape, which is typical for electrical double layer capacitors (EDLCs).[43−45] The IR-CNT yarn supercapacitor, on the other hand, showed a significantly higher current density than the as-spun CNT yarn supercapacitor with peaks that are usually associated with redox reactions displayed by pseudocapacitance materials. These peaks may be attributed to the oxygen groups introduced by gamma irradiation treatment,[27] in a similar way as the origination of faradaic reactions from oxygen and nitrogen heteroatoms in conventional carbon materials.[20−23,46] Figure 3b presents the galvanostatic charge−discharge curves of the two supercapacitors measured at a constant current density of 0.2 A· g^{-1}. The charge and discharge times of the IR-CNT yarn supercapacitor were considerably longer than that of the as-spun CNT yarn supercapacitor, indicating a significant improvement of capacitance.

The two supercapacitors were further characterized using electrochemical impedance spectroscopy (EIS), from which Nyquist plots were obtained. The two curves in Figure 3c almost coincide each other at low frequency range. Enlargements of the Nyquist plots (Figure 3d) show the impedances of the two supercapacitors at high frequency range. The x-intercept of the Nyquist plot represents the equivalent series resistance (ESR) that corresponds to charge transport resistance for the two-electrode supercapacitor.[34] The IR-CNT yarn supercapacitor had less than a half of the ESR of the as-spun CNT yarn supercapacitor. This is consistent with the increased electrical conductivity of the IR-CNT yarn measured by the four-probe method mentioned above.

3.3. Carbon Nanotube Yarn As a Substrate for Polyaniline Nanowire Supercapacitor. The as-spun CNT yarn and IR-CNT yarn were coated in polyaniline nanowire solution using the continuous coating and drying device shown in Figure 2. The PANI take-up in the two coated yarns after drying was controlled to approximately the same (∼10 wt %). Figure 4 shows the surface morphology of the as-spun CNT, IR-CNT and IR-CNT@PANI yarns. The carbon nanotubes are well aligned along the twist helices. No noticeable morphological difference was found between the as-spun CNT yarn and the gamma-irradiated IR-CNT yarn. The diameter of the pure CNT yarn was approximately 25 μm.

dx.doi.org/10.1021/am404967x | ACS Appl. Mater. Interfaces 2014, 6, 2553−2560

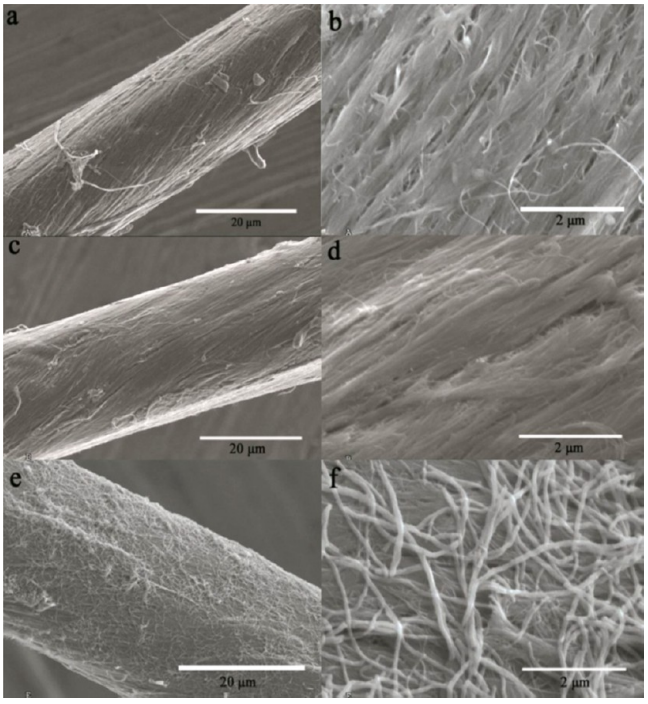

Figure 4. SEM images of single yarns used in the two-ply yarn supercapacitors: (a, b) as-spun CNT yarn, (, d) gamma irradiated yarn (IR-CNT), (e, f) gamma-irradiated CNT yarn deposited with polyaniline nanowires (IR-CNT@PANI).

The application of PANI coating did not change the yarn diameter significantly because of the relatively small take-up rate. As shown in images e and f in Figure 4, the PANI nanowires on the yarn surface have diameters ranging from about 20 to 50 nm and lengths around 2−5 μm. They form a mesh structure with some intermingling with the carbon nanotubes on the yarn surface. The random orientation of the PANI nanowires is distinctly different from the vertically aligned PANI nanowires prepared by in situ dilute polymerization method reported previously.[34] Besides SEM examination, the presence of PANI on the IR-CNT@PANI yarn was confirmed using FT-IR and Raman spectroscopy analyses, which are given as Supporting Information.

Coating of PVA-H_3PO_4 gel increased the yarn diameter from 25 to 35 μm, giving a 5 μm average thickness of coated layer on the yarn surface. The final two-ply yarn supercapacitors were still much finer than fine count textile yarns (compare the two-ply yarn supercapacitor shown in Figure 1c with the fine count cotton yarn shown in Figure 1d).

The electrochemical performances of the two-ply yarn supercapacitors made from the CNT@PANI and IR-CNT@PANI yarns are shown in Figure 5 together with the results of the two supercapacitors based on as-spun CNT yarn and IR-CNT yarn presented earlier. Additional galvanostatic charge−discharge curves over a wide range of current densities and additional CV curves over a wide range of scan rates for the IR-CNT@PANI two-ply yarn supercapacitor are provided in Figure 6.

Figure 5a shows the CV curves of the four types of supercapacitors carried out at the scanning rate of 0.5 V s^{-1} in the potential range from 0 to 1.0 V. The CNT@PANI and IR-CNT@PANI supercapacitors showed much wider windows than the other two supercapacitors that were not incorporated with polyaniline nanowires. The supercapacitors coated with polyaniline nanowires showed strong redox peaks at all scan rates (Figure 6), reflecting the nature of the high-performance pseudocapacitance polyaniline nanowires.[47] The galvanostatic charge−discharge curves of the four supercapacitors are compared in Figure 5b. With the incorporation of polyaniline nanowires, the charge/discharge times were dramatically extended and the charge−discharge curves demonstrated curved triangle shapes.

The gram capacitances of all the four supercapacitors in Figure 5c showed a small initial decline and then stabilization as current density increased. We can observe a significant effect attributable to the incorporation of PANI nanowires by comparing the as-spun CNT yarn supercapacitor with the CNT@PANI yarn supercapacitor, and by comparing IR-CNT with IR-CNT@PANI. The IR-CNT@PANI supercapacitor showed a 10-fold improvement in gram capacitance over the IR-CNT yarn supercapacitor (7.5 F g^{-1}, at current density 2.0 A g^{-1}), whereas the CNT@PANI yarn supercapacitor showed a 7-fold improvement over the as-spun CNT yarn supercapacitor (4.8 F g^{-1}). A significant improvement attributable to gamma irradiation treatment can also be found. The IR-CNT@PANI supercapacitor showed a gram capacitance of 78 F g^{-1} at current density 2.0 A g^{-1}, which was more than twice as much as that of the CNT@PANI yarn supercapacitor (35.2 F· g^{-1}).

The gram capacitance of the IR-CNT@PANI two-ply yarn supercapacitor was considerably higher than most threadlike supercapacitors reported recently, including supercapacitors based on hybrid polypyrrole (PPy)-multi walled carbon nanotube yarn (60 F g^{-1}),[36] and the all graphene fiber-based supercapacitors (25−40 F g^{-1}).[48] The gram capcitance of 78 F g^{-1} for the IR-CNT@PANI supercapacitor can be converted into an area capacitance of 43 mF cm^{-2}, which was higher than the value found in the two-ply yarn supercapacitor based on as-spun CNT yarn and vertically aligned polyaniline nanowire arrays prepared using a sophisticated in situ polymerization process.[34] In addition, the IR-CNT@PANI yarn supercapacitor reported here virtually eliminated the problem of rapid decrease in capacitance at high current density shown by the previous supercapacitor.[34]

The Nyquist plots of the four types of supercapacitors derived from electrochemical impedance spectroscopy are compared in Figure 5d. The inset in Figure 5d shows that the equivalent series resistances (ESR) of the two supercapacitors made from gamma-irradiated yarns (IR-CNT and IR-CNT@PANI) were considerably lower than that of the two supercapacitors made from the unirradiated yarns (CNT and CNT@PANI).

Conducting polymers such as polyaniline suffer from poor cyclic stability as electrode materials for supercapacitors because of the mechanical stress caused by material swelling and shrinking during the charge−discharge process.[49] The cyclic charge−discharge stability of the four types of two-ply yarn supercapacitors at 1.0 A g^{-1} are shown in Figure 5e. The pure CNT and IR-CNT yarn supercapacitors showed very little reduction in capacitance after 1000 charge−discharge cycles. The CNT@PANI and IR-CNT@PANI supercapacitors also displayed high cyclic stability, with the IR-CNT@PANI yarn supercapacitor showing a capacitance retention ratio of 89% after 1000 cycles. This indicates that the CNT yarn, with and without the gamma irradiation treatment, provides an excellent reinforcement for the PANI nanowires.

Threadlike supercapacitors for wearable electronics must also possess excellent flexibility without sacrificing their electro-

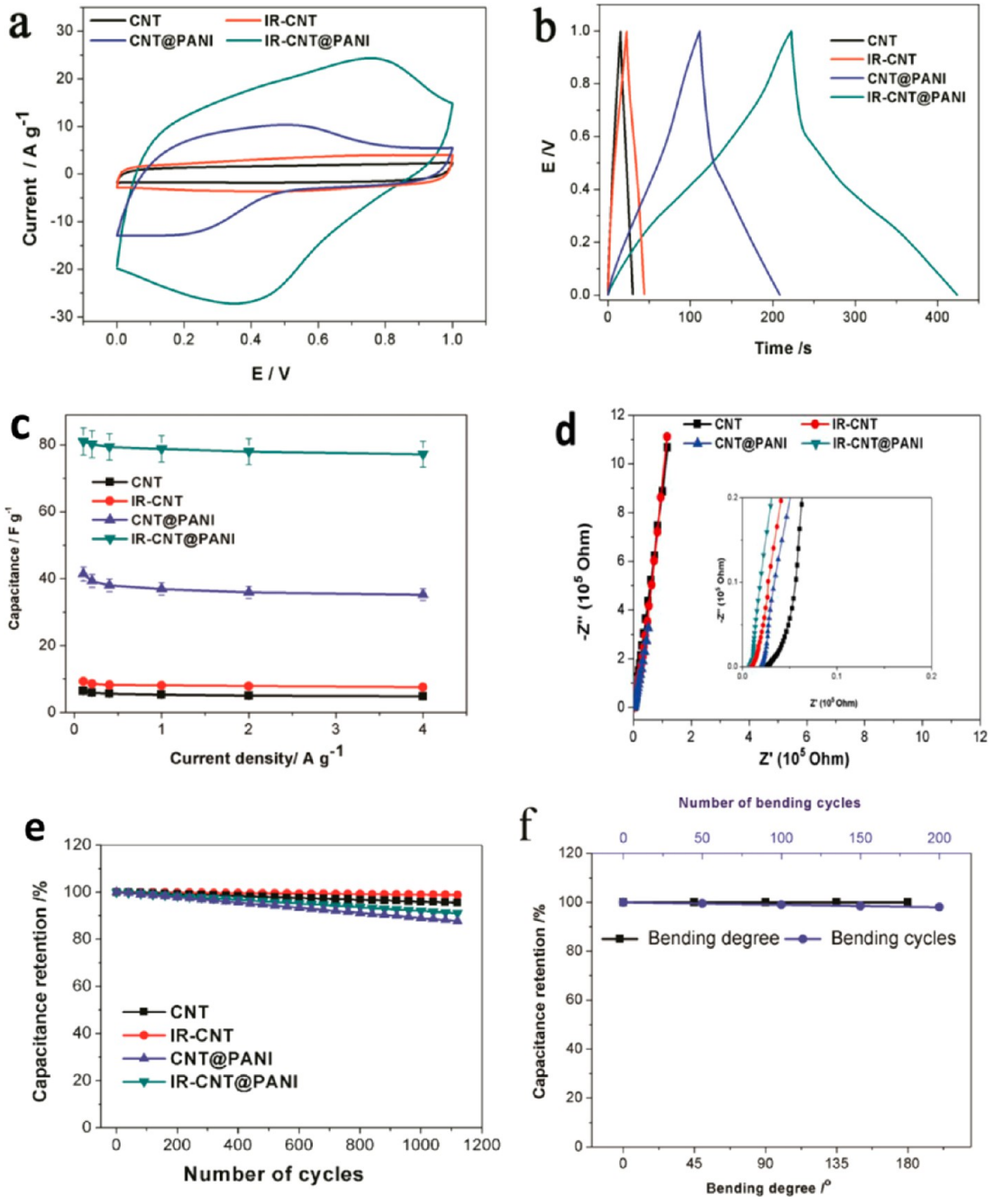

Figure 5. Electrochemical properties of all four types of two-ply yarn supercapacitors. (a) Cyclic voltammograph (CV) curves at scan rate 0.5 V s^{-1}. (b) Galvanostatic charge/discharge curves at current density 0.2 A g^{-1}. (c) Gram capacitances at different current densities. (d) Impedance spectroscopy with a frequency loop from 500 kHz to 10 mHz using a perturbation amplitude of 5 mV at open-circuit potential. (e) Cyclic charge–discharge stability at current density of 1.0 A g^{-1}. (f) Capacitance retention ratios after different bending degrees and number of bending cycles derived from galvanostatic charge/discharge experiments at current density 1.0 A g^{-1}.

chemical performance. As shown in Figure 5f, the angle of bending had practically no effect on the capacitance of the IR-CNT@PANI supercapacitor. The capacitance of the supercapacitor was little affected by repeated folding (180° bending) and unfolding actions, showing a 2% loss in capacitance after 200 folding–unfolding cycles.

4. CONCLUSIONS

Carbon nanotube yarn is an attractive choice of substrate material for linear (fiber or yarn) supercapacitors used in wearable electronic textiles because of its high strength, flexibility, electrical conductivity, and structural porosity. The as-spun CNT yarn on its own behaves like a typical electrical double-layer capacitor. Oxidation of the carbon nanotube yarn by gamma irradiation treatment in the presence of oxygen can significantly increase the specific capacitance of the yarn. This improvement can be attributed to the pseudocapacitance characteristics introduced by functional groups developed in the irradiation treatment, in addition to the increases in tensile strength and electrical conductivity. The gamma-irradiated carbon nanotube yarn can therefore be used as a strong reinforcement and highly efficient current collector for

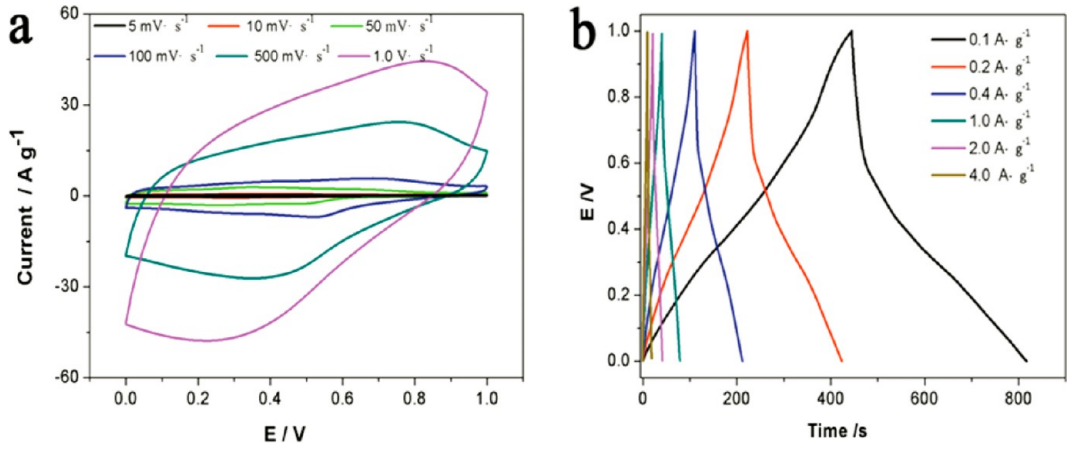

Figure 6. Electrochemical performance of the IR-CNT@PANI yarn supercapacitor. (a) Cyclic voltammograms at different scan rates 5, 10, 50, 100, 500, 1000 mV s^{-1}. (b) Galvanostatic charge/discharge curves at different current densities 0.1, 0.2, 0.4, 1, 2, 4 A g^{-1}.

threadlike supercapacitors made from high performance pseudocapacitance materials. The two-ply yarn supercapacitor based on gamma-irradiated CNT yarn and randomly orientated polyaniline nanotwires demonstrated excellent specific capacitance and maintained its capacitance very well at high current densities. It has shown the high cyclic charge−discharge stability, high flexibility, and high strength that are required for wearable electronics.

■ ASSOCIATED CONTENT

Ⓢ Supporting Information

FTIR spectra of polyaniline nanowires and IR-CNT@PANI yarn, and Raman spectra of polyaniline nanowires and IR-CNT@PANI yarn. This material is available free of charge via the Internet at http://pubs.acs.org.

■ AUTHOR INFORMATION

Corresponding Author

*E-mail: menghe.miao@csiro.au. Tel: +61 3 5246 4000. Fax: +61 3 5246 4047.

Notes

The authors declare no competing financial interest.

■ ACKNOWLEDGMENTS

We are thankful for the assistance of Chi Huynh, Margret Pate, and Colin Veitch in this work. F.S. acknowledges China Scholarship Council for granting a visiting scholarship that enabled him to carry out this work at CSIRO Materials Science and Engineering in Australia.

■ REFERENCES

(1) Pushparaj, V. L.; Shaijumon, M. M.; Kumar, A.; Murugesan, S.; Ci, L.; Vajtai, R.; Linhardt, R. J.; Nalamasu, O.; Ajayan, P. M. *Proc. Natl. Acad. Sci. U.S.A.* **2007**, *104*, 13574−13577.
(2) Wang, D.-W.; Li, F.; Zhao, J.; Ren, W.; Chen, Z.-G.; Tan, J.; Wu, Z.-S.; Gentle, I.; Lu, G. Q.; Cheng, H.-M. *ACS Nano* **2009**, *3*, 1745−1752.
(3) Torop, J.; Palmre, V.; Arulepp, M.; Sugino, T.; Asaka, K.; Aabloo, A. *Carbon* **2011**, *49*, 3113−3119.
(4) Zhang, J.; Wang, Y.; Zang, J.; Xin, G.; Yuan, Y.; Qu, X. *Carbon* **2012**, *50*, 5196−5202.
(5) Cai, F.; Chen, T.; Peng, H. *J. Mater. Chem.* **2012**, *22*, 14856−14860.
(6) Salinas-Torres, D.; Sieben, J. M.; Lozano-Castelló, D.; Cazorla-Amorós, D.; Morallón, E. *Electrochim. Acta* **2013**, *89*, 326−333.
(7) Cao, J.; Safdar, M.; Wang, Z.; He, J. *J. Mater. Chem. A* **2013**, *1*, 10024−100029.
(8) Qian, H.; Diao, H.; Shirshova, N.; Greenhalgh, E. S.; Steinke, J. G. H.; Shaffer, M. S. P.; Bismarck, A. *J. Colloid Interface Sci.* **2013**, *395*, 241−248.
(9) Masarapu, C.; Zeng, H. F.; Hung, K. H.; Wei, B. *Acs Nano* **2009**, *3*, 2199−2206.
(10) Fan, Z.; Yan, J.; Zhi, L.; Zhang, Q.; Wei, T.; Feng, J.; Zhang, M.; Qian, W.; Wei, F. *Adv. Mater.* **2010**, *22*, 3723−8.
(11) Frackowiak, E.; Béguin, F. *Carbon* **2001**, *39*, 937−950.
(12) Miao, M. *Particuology* **2013**, *11*, 378−393.
(13) Miao, M. *Carbon* **2012**, *50*, 4973−4983.
(14) Ouyang, J.; Chu, C. W.; Chen, F. C.; Xu, Q.; Yang, Y. *Adv. Funct. Mater.* **2005**, *15*, 203−208.
(15) Choi, K. S.; Liu, F.; Choi, J. S.; Seo, T. S. *Langmuir* **2010**, *26*, 12902−12908.
(16) Lang, U.; Naujoks, N.; Dual, J. *Synth. Met.* **2009**, *159*, 473−479.
(17) Chen, C.-h.; Torrents, A.; Kulinsky, L.; Nelson, R. D.; Madou, M. J.; Valdevit, L.; LaRue, J. C. *Synth. Met.* **2011**, *161*, 2259−2267.
(18) Lee, J. A.; Shin, M. K.; Kim, S. H.; Cho, H. U.; Spinks, G. M.; Wallace, G. G.; Lima, M. D.; Lepró, X.; Kozlov, M. E.; Baughman, R. H.; Kim, S. J. *Nat. Commun.* **2013**, *4*, 1970.
(19) Dai, L.; Chang, D. W.; Baek, J. B.; Lu, W. *Small* **2012**, *8*, 1130−66.
(20) Frackowiak, E. In *Supercapacitors*; Wiley−VCH: Weinhein, Germany, 2013; pp 207−237.
(21) Kötz, R.; Carlen, M. *Electrochim. Acta* **2000**, *45*, 2483−2498.
(22) Momma, T.; Liu, X.; Osaka, T.; Ushio, Y.; Sawada, Y. *J. Power Sources* **1996**, *60*, 249−253.
(23) Hsieh, C.-T.; Teng, H. *Carbon* **2002**, *40*, 667−674.
(24) Ishikawa, M.; Sakamoto, A.; Monta, M.; Matsuda, Y.; Ishida, K. *J. Power Sources* **1996**, *60*, 233−238.
(25) Filleter, T.; Espinosa, H. D. *Carbon* **2013**, *56*, 1−11.
(26) Skakalova, V.; Dettlaff-Weglikowska, U.; Roth, S. *Diamond Relat. Mater.* **2004**, *13*, 296−298.
(27) Miao, M.; Hawkins, S. C.; Cai, J. Y.; Gengenbach, T. R.; Knott, R.; Huynh, C. P. *Carbon* **2011**, *49*, 4940−4947.
(28) Skakalova, V.; Hulman, M.; Fedorko, P.; Lukáč, P.; Roth, S. *AIP Conf. Proc.* **2003**, 143.
(29) Peng, B.; Locascio, M.; Zapol, P.; Li, S.; Mielke, S. L.; Schatz, G. C.; Espinosa, H. D. *Nat. Nanotechnol.* **2008**, *3*, 626−631.
(30) Kis, A.; Csányi, G.; Salvetat, J. P.; Lee, T.-N.; Couteau, E.; Kulik, A. J.; Benoit, W.; Brugger, J.; Forró, L. *Nat. Mater.* **2004**, *3*, 153−157.
(31) Rahy, A.; Yang, D. J. *Mater. Lett.* **2008**, *62*, 4311−4314.
(32) Yang, J. E.; Jang, I.; Kim, M.; Baeck, S. H.; Hwang, S.; Shim, S. E. *Electrochim. Acta* **2013**, *111*, 136−143.
(33) Gupta, V.; Miura, N. *Electrochem. Solid-State Lett.* **2005**, *8*, A630−A632.

(34) Wang, K.; Meng, Q.; Zhang, Y.; Wei, Z.; Miao, M. *Adv. Mater.* **2013**, *25*, 1494−8.
(35) Ren, J.; Li, L.; Chen, C.; Chen, X.; Cai, Z.; Qiu, L.; Wang, Y.; Zhu, X.; Peng, H. *Adv. Mater.* **2013**, *25*, 1155−1159.
(36) Foroughi, J.; Spinks, G. M.; Ghorbani, S. R.; Kozlov, M. E.; Safaei, F.; Peleckis, G.; Wallace, G. G.; Baughman, R. H. *Nanoscale* **2012**, *4*, 940−945.
(37) Huynh, C. P.; Hawkins, S. C. *Carbon* **2010**, *48*, 1105−1115.
(38) Miao, M.; McDonnell, J.; Vuckovic, L.; Hawkins, S. C. *Carbon* **2010**, *48*, 2802−2811.
(39) Miao, M. *Carbon* **2011**, *49*, 3755−3761.
(40) Lei, Z.; Zhang, J.; Zhao, X. S. *J. Mater. Chem.* **2012**, *22*, 153.
(41) Cai, Y.; Cui, X.; Rodgers, J.; Thibodeaux, D.; Martin, V.; Watson, M.; Pang, S.-S. *Text. Res. J.* **2013**, *83*, 961−970.
(42) Li, B.; Feng, Y.; Ding, K.; Qian, G.; Zhang, X.; Zhang, J. *Carbon* **2013**, *60*, 186−192.
(43) Zhai, Y.; Dou, Y.; Zhao, D.; Fulvio, P. F.; Mayes, R. T.; Dai, S. *Adv. Mater.* **2011**, *23*, 4828−4850.
(44) Chen, J. H.; Li, W. Z.; Wang, D. Z.; Yang, S. X.; Wen, J. G.; Ren, Z. F. *Carbon* **2002**, *40*, 1193−1197.
(45) Yoon, B.-J.; Jeong, S.-H.; Lee, K.-H.; Seok Kim, H.; Gyung Park, C.; Hun Han, J. *Chem. Phys. Lett.* **2004**, *388*, 170−174.
(46) Frackowiak, E.; Delpeux, S.; Jurewicz, K.; Szostak, K.; Cazorla-Amoros, D.; Béguin, F. *Chem. Phys. Lett.* **2002**, *361*, 35−41.
(47) Rudge, A.; Davey, J.; Raistrick, I.; Gottesfeld, S.; Ferraris, J. P. *J. Power Sources* **1994**, *47*, 89−107.
(48) Meng, Y.; Zhao, Y.; Hu, C.; Cheng, H.; Hu, Y.; Zhang, Z.; Shi, G.; Qu, L. *Adv. Mater.* **2013**, *25*, 2326−2331.
(49) Bélanger, D.; Ren, X.; Davey, J.; Uribe, F.; Gottesfeld, S. *J. Electrochem. Soc.* **2000**, *147*, 2923−2929.